

**Giant Gating Tunability of Optical Refractive Index in Transition Metal
Dichalcogenide Monolayers**

Yiling Yu^{1,2}, Yifei Yu¹, Lujun Huang¹, Haowei Peng³, Liwei Xiong^{1,4} and Linyou Cao^{1,2*}

¹Department of Materials Science and Engineering, North Carolina State University, Raleigh NC 27695; ²Department of Physics, North Carolina State University, Raleigh NC 27695;

³Department of Chemistry, Temple University, Philadelphia PA 19405;

⁴Hubei Key Laboratory of Plasma Chemistry and Advanced Materials, Wuhan Institute of Technology, Wuhan, PR China, 430205.

* To whom correspondence should be addressed.

Email: lcao2@ncsu.edu

This PDF document includes

Experimental Methods

Figure S1-S8

S1. Fitting dielectric function using a multi-Lorentzian model

S2. Design optical absorption modulator

Table S1

Experimental methods

The Raman and PL measurement were carried out at Horiba Labram HR800 system with incident wavelength of 532 nm. The reflection spectra were collected using a home-built setup that consists of a confocal microscope (Nikon Eclips C1) connected with a monochromator (SpectraPro, Princeton Instruments) and a detector (Pixis, Princeton Instruments). A broadband Halogen lamp was used as incident light for the reflection measurements. The reflectance from the sample is calculated by normalizing the light reflected from sample with respect to the light reflected from a dielectric mirror under the same configuration.

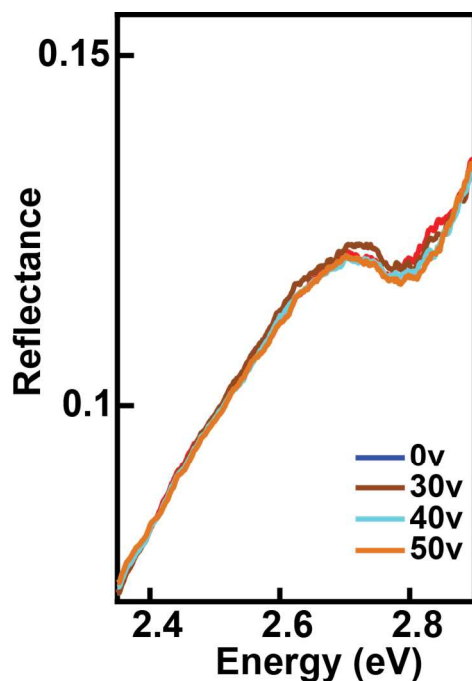


Figure S1 Negligible dependence in the reflection efficiency of the C exciton of monolayer WS₂ on electrical gating.

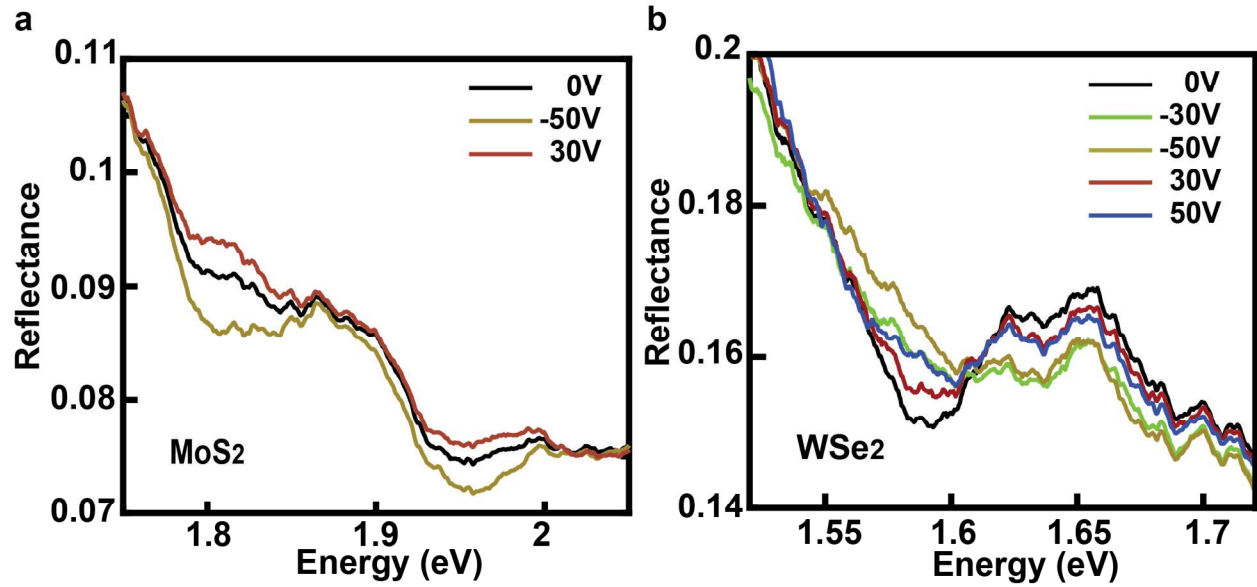


Figure S2. Spectral reflection collected from (a) monolayer MoS₂ and (b) monolayer WSe₂ under different gating voltages.

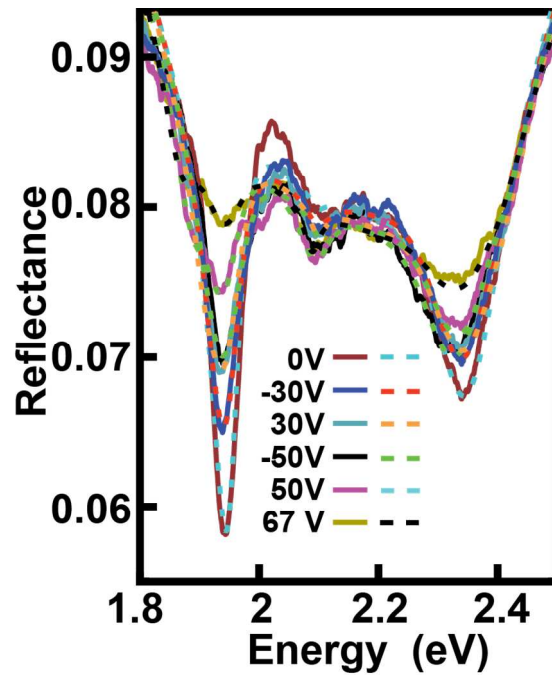


Figure S3. Fitted (dash lines) and measured (solid lines) spectra reflection of monolayer WS₂ under different gate voltages. In this fitting, the dielectric function is fitted using the multi Lorentzian model.

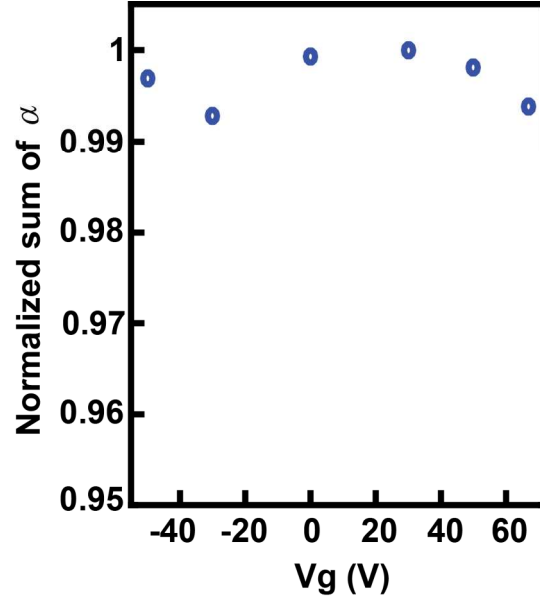


Figure S4. The sum of the absorption coefficient $\int_0^{6\text{eV}} \alpha(\omega)$ at different gating voltages. The result is normalized with respect to the sum of absorption coefficient at 0V.

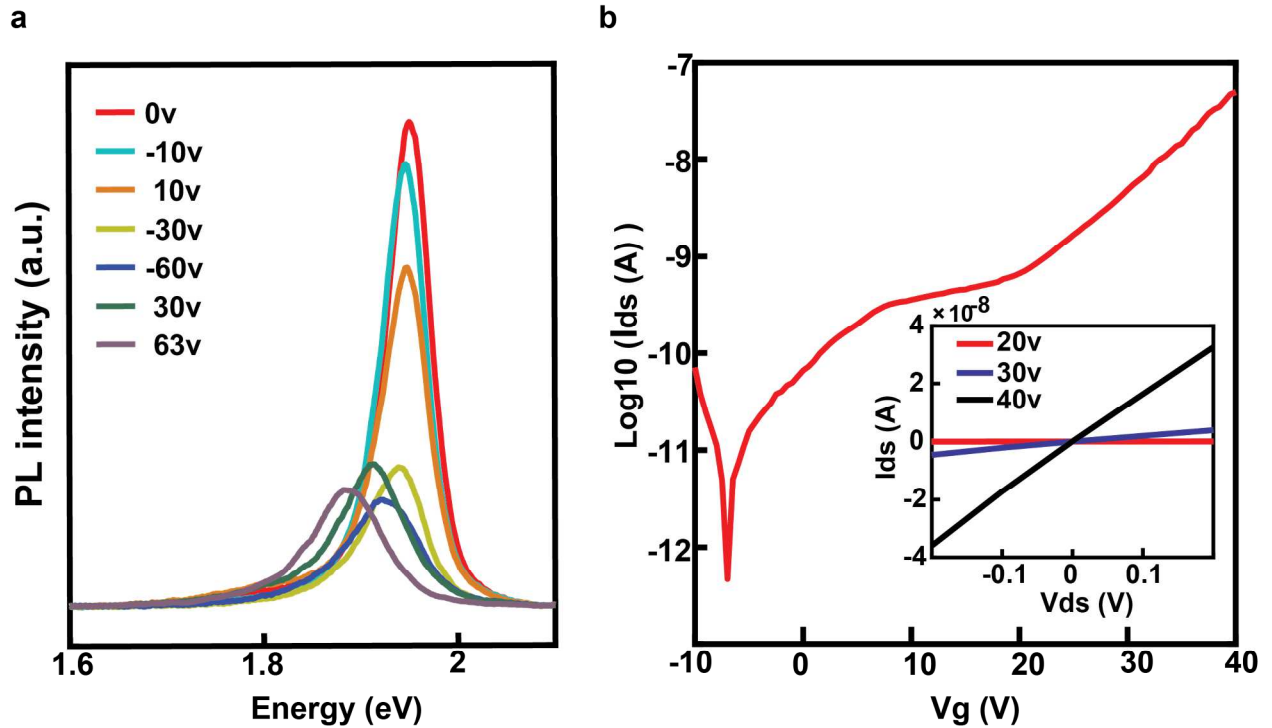


Figure S5. (a) Photoluminescence spectra of monolayer WS₂ under different gate voltages. (b) I-V curve measurement of monolayer WS₂. The inset is I-V curve of drain-source electrodes under different back gate voltages (V_g). The linear relation indicates good Ohmic contacts.

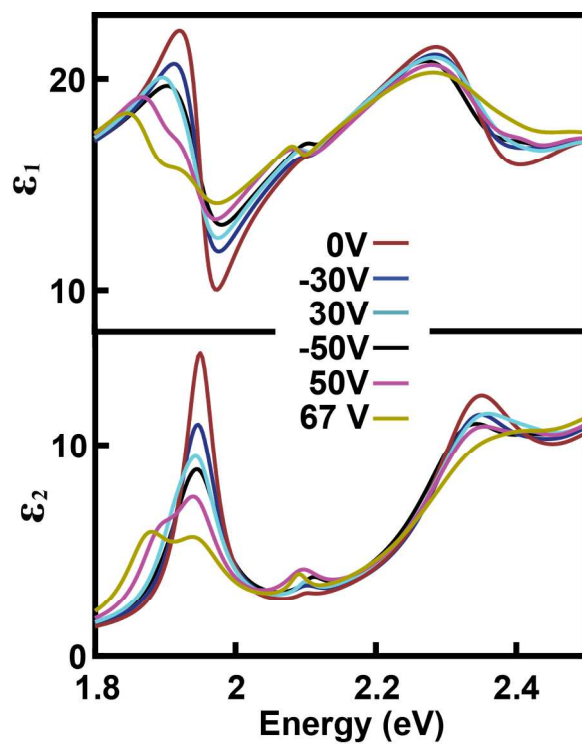


Figure S6 Fitted real (upper) and imaginary (lower) parts of dielectric function under different gate voltages.

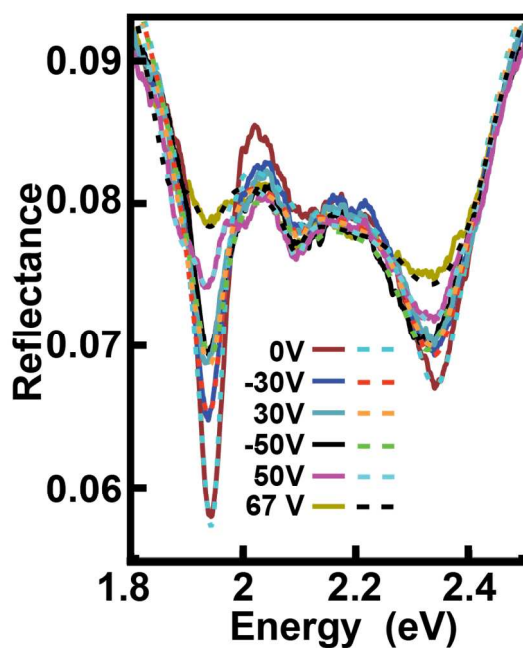


Figure S7. Fitted (dash lines) and measured (solid lines) spectra reflection of monolayer WS_2 under different gate voltages. The dielectric function is fitted using the Fractional dimensional space model.

S1. Fitting dielectric function using a multi-Lorentzian model

In order to get accurate determination of the dielectric function ε , the Kramers-Kronig constrained analysis requires information in the full spectral range, but the measured spectral reflection only cover the range of 1.8-2.5 eV. To address this issue, we ignore the contribution from the oscillators in lower energy ranges as it is expected to be weak for the refractive index in the visible range. However, the contribution from the oscillators at higher energy ranges has to be considered. We assume that the dielectric function of the monolayer at the higher energy ranges is similar to that of bulk counterparts, and use the dielectric function of the bulk counterparts, which is available in reference (Ref. 27 in the main text), to correct the oscillators of the monolayers in the higher energy range. Multiple oscillators are set with equal space of 0.1eV and almost equal damping constant 0.3eV. The oscillation strength of these oscillators is fitted to match the dielectric function of bulk WS₂ in the UV frequency range. The high frequency Lorentzian oscillators are fitted up to 6eV. The contribution from even higher frequency (larger than 6eV and up to infinite frequency) oscillators are put into ε_{∞} . Different sets of oscillation parameters and ε_{∞} have been evaluated to get good matches to both the measured reflection spectrum in visible range (Fig. 1a) and refractive index of bulk WS₂ in UV frequency range.

To further exam the accuracy of the fitting method, we measured the refractive index of monolayer WS₂ film using standard spectral ellipsometry, and compared it to the refractive index obtained from the fitting of spectral reflection. The two sets of refractive index show nice consistence, with a difference 0f 0.3 and 0.2 in the real and imaginary parts around exciton resonance as indicated by Fig. S8.

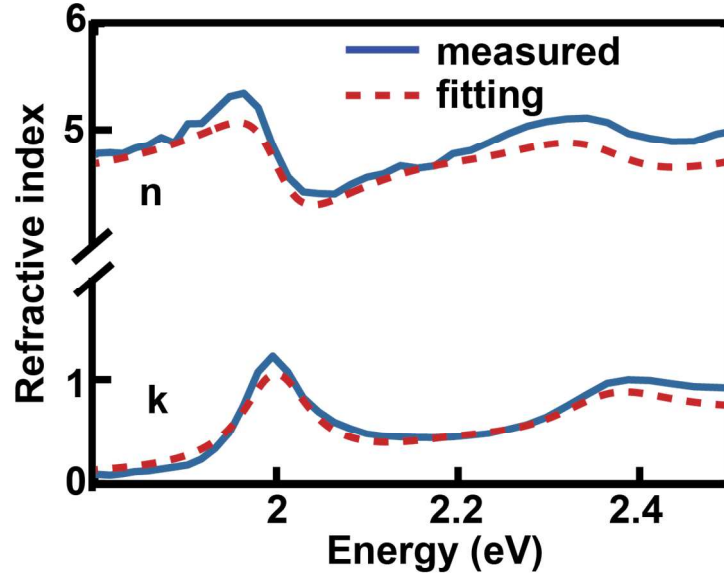


Figure S8 Measured (blue solid lines) and fitted (red dash lines) refractive index of monolayer WS₂ film, (upper) real and (lower) imaginary parts of the refractive index.

Table S1. Parameters used in the calculation for the thermal equilibrium of neutral and charged excitons

$n_{+/-}(\text{cm}^{-2})$	$+8.1 \times 10^{12}$	$+4.5 \times 10^{12}$	-9×10^{11}	-6.5×10^{12}	-10.3×10^{12}	-13.7×10^{12}
$E_{A0} - E_{A+/-}$ (meV)	23.0	13.0	24.0	37.0	53.0	65.0
E_F (meV)	20.8	11.6	3.0	20.7	32.8	43.6
$E_{b+/-}$ (meV)	2.2	1.4	21	16.3	20.2	21.4

Note: ‘+’ denote hole doping and ‘-’ denote electron doping. The unit is meV. The binding energy of the charged A exciton can be calculated as $E_{A0} - E_{A+/-} - E_F$, where E_{A0} and $E_{A+/-}$ are the optical bandgap of the neutral and charged A excitons, respectively. E_F is the fermi energy shift with respect to the minimum of conduction band caused by the injected charge carriers. It can be calculated from the charge density n and the density of state in 2D system as $E_F = \hbar^2 \pi n / 2m^*$. The effective electron mass $0.35m_0$ and effective hole mass $0.46m_0$ are used for calculating E_F . ^{S1} m_0 is the free electron mass.

S2. Design optical absorption modulator

The device design is focused on the spectral range around the A excitonic peak, which is 1.956 eV. Without losing generality, we use two charge densities as examples to illustrate the device design, $-0.9 \times 10^{12} \text{ cm}^{-2}$ and $-13.7 \times 10^{12} \text{ cm}^{-2}$. The refractive index of monolayer WS_2 in the target spectral range (1.956 eV) is $4-1.698i$ at $-0.9 \times 10^{12} \text{ cm}^{-2}$ and $3.86-0.6885i$ at $-13.7 \times 10^{12} \text{ cm}^{-2}$. The design follows a theoretical frame of leaky mode coupling that we have previously developed. [Ref 45]. To ensure the optical resonance in the wavelength of interest, $\sim 600\text{nm}$, we choose 140nm thick GaN nanowire array on sapphire substrate with Ag mirror coated on the back side). 10nm thick HfO_2 is deposit on top of GaN as gate dielectrics. The monolayer WS_2 may be transferred onto the top of the nanostructure (Fig. 5(a)). The refractive index for the HfO_2 and GaN are 2.1 and 2.35, respectively. Our simulation results (Fig. 5(b)) show that the absorption efficiency around 1.956eV is 80% at condition1 (carrier concentration $-0.9 \times 10^{12} \text{ cm}^{-2}$) but with only 40% absorption efficiency for condition2 ($-13.7 \times 10^{12} \text{ cm}^{-2}$). This really suggests a large absorption and reflection modulation can be achieved by electrical gating monolayer WS_2 .

References

[S1] L. Liu, S. Bala Kumar, Y. Ouyang, and J. Guo. *IEEE Trans. Electron Devices*, **2011**, 58, 3042–3047

